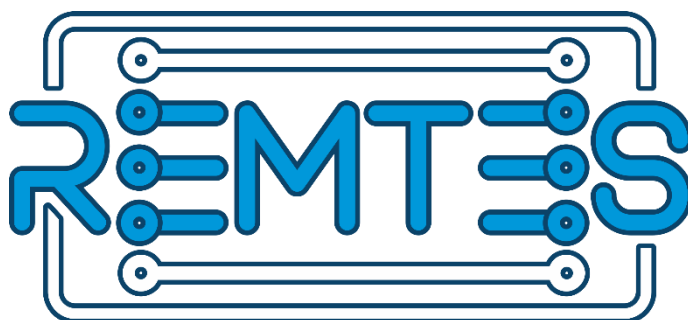




REMTES
TECHNOLOGY FOR REMOTE TEMPERATURE
MEASUREMENTS IN MICROFLUIDIC DEVICES

PROGRAM-PRIZMA-2023-2026
Grant Agreement: 7017



Deliverable 1.2.
Double-activated and upconverted
luminescence thermal probes
Version Final

Project Deliverable Information Sheet

REMTES Project	Project Ref. No. 7017
	Project Title: Technology for remote temperature measurements in microfluidic devices
	Project Website: https://www.remtes-prizma.org
	Deliverable No.: D 1.2
	Deliverable Type: Report
	Month of delivery: 18
	Actual Delivery Date: 31/05/2025
	Principal investigator: Miroslav Dramićanin

Document Control Sheet

Document	Title: Double-activated and upconverted luminescence thermal probes.docx
	Version Final
	Distributed to REMTES Participants and through Project Website
Authorship	Written by Željka Antić
	Contributed by Tatjana Dramićanin, Bojana Milićević, Sanja Kuzman, Ljubica Đačanin Far, Katarina Milenković
	Reviewed by Miroslav Dramićanin
	Approved by Miroslav Dramićanin

History of Changes

Version	Date	Description	Reviewer
V0	05.05.2025.	Version 0	Željka Antić
V1	20.05.2025.	Version 1	Tatjana Dramićanin, Bojana Milićević, Sanja Kuzman, Ljubica Đačanin Far, Katarina Milenković
V2	31.05.2025.	Version Final	Miroslav Dramićanin

Table of Contents

INTRODUCTION	4
D2.1: Double-activated and upconverted luminescence thermal probes	5
1. YAG:Er ³⁺ /Mn ⁴⁺ thermal probe.....	5
1.1. Experimental part	5
1.2. Phase & Morphological analysis.....	5
1.3. Photoluminescence of YAG:Er ³⁺ /Mn ⁴⁺	6
1.4. Luminescence thermometry of YAG:Er ³⁺ /Mn ⁴⁺	7
2. YAG:Yb ³⁺ /Ce ⁴⁺ thermal probe	9
2.1. Experimental part	9
2.2. Phase & Structural analysis.....	9
1.1. UV-VIS diffuse reflectance of YAG:Yb ³⁺ /Ce ⁴⁺	10
References.....	11

Copyright Notice

Copyright © 2024 REMTES project team. All rights reserved. REMTES is a project funded by the Science Fund of the Republic of Serbia under grant agreement no. 7017. For more information on the project and contributors please see <http://www.remtes-prizma.org/>. It is allowed to copy and distribute verbatim copies of this document containing this copyright notice; however, the modification of this document is forbidden.

Disclaimer

Vinča Institute is solely responsible for the content of this publication, and this content does not express the views of the Science Fund of the Republic of Serbia.

INTRODUCTION

REMTES – “Technology for remote temperature measurements in microfluidic devices” is a Science Fund of the Republic of Serbia funded project (Program PRIZMA, Grant Contract No. 7017) coordinated and completely executed by "Vinča" Institute of Nuclear Sciences – National Institute of the Republic of Serbia, University of Belgrade (VINS). The project will run from December 1st 2023 to November 30th 2026.

REMTES is a highly ambitious and innovative project aimed at developing a breakthrough system for measuring sample temperatures on the nanoliter scale. The project will develop an optical self-referencing thermometer for use in micro- and nanofluidics in the 0–100 °C temperature range by exploiting temperature-induced changes in the luminescence of materials and nanomaterials; that is, by advancing luminescence (nano-) thermometry in a targeted manner. The project aims to go beyond the state of the art and implement a radically new technology that merges the fields of luminescence thermometry, photothermal spectroscopy, and microfluidics to develop new-generation luminescent thermometry probes using cutting-edge luminescent, temperature-sensitive, and chemically stable inorganic materials in bulk and nanomaterial forms. The probes will be embedded in microfluidic chip channels to enable self-referenced remote temperature measurements, and the technology will be validated by a portable microfluidic luminescent thermometer, as well as in-situ temperature measurements of fluid flow in nanoliter volume samples. Multiple conceptual breakthroughs can be further envisaged from the proposed technology credibly spreading its impact to multiple technological areas.

The present document – **D1.2: Double-activated and upconverted luminescence thermal probes** is a deliverable of the WP1 of the REMTES project. A report describes the double-activated and upconverted luminescence thermal probes, with their basic structural, morphological, and luminescence features. This is the result of a joint effort between WP1, WP2, and WP3. Up to four probes will be selected for further implementation in a microfluidic device with an integrated luminescence thermometer.

D2.1: Double-activated and upconverted luminescence thermal probes

Starting from the project beginning up to the end of the first project year, REMTES team members under SUBACTIVITY 1.3: DOUBLE-ACTIVATED INORGANIC LUMINESCENCE THERMAL PROBES; SUBACTIVITY 1.4. INORGANIC UPCONVERSION LUMINESCENCE THERMAL PROBES; AND SUBACTIVITY 2.1: STRUCTURAL, MORPHOLOGICAL, and THERMAL PROPERTIES OF LUMINESCENT PROBES designed, synthesized and structurally, morphologically and optically characterized following double-activated and upconverted luminescence thermal probes:

1. YAG:Er³⁺/Mn⁴⁺ thermal probe

1.1. Experimental part

Following chemicals commercially available: metal nitrate salts (yttrium(III) nitrate hexahydrate, Y(NO₃)₃×6H₂O; manganese (II) nitrate tetrahydrate, Mn(NO₃)₂×4H₂O; europium (III)-nitrate pentahydrate, Eu(NO₃)₃×5H₂O; aluminium (III) nitrate nonahydrate, Al(NO₃)₃×9H₂O; Alfa Aesar, purity 99.9%, 99.99+, 99.9%, 98+%, respectively); citric acid - CA (HOC(COOH)(CH₂COOH)₂, Sigma Aldrich, ACS reagent, ≥99.5%) and ethylene glycol - EG (HOCH₂CH₂OH, Sigma Aldrich, anhydrous, 99.8%) were used as purchased.

In this work: Y₃Al₅O₁₂:1 mol% Er³⁺, 0.5 mol% Mn⁴⁺ sample was synthesized by Pechini method (sample formula-Y_{2.97}Er_{0.03}Al_{4.975}Mn_{0.025}O₁₂; abbreviated name YAG:1Er0.5Mn). The concentrations of rare earth and transition metal ions have been chosen arbitrary based on our previous experience with double activated garnets. The sample has been synthesized from metal nitrates dissolved in the solution of CA and EG. Detailed method is given in the work earlier printed by our research group [1]. The acquired sample in a form of yellow gel was temperature treated in two steps: calcination at 600°C for 2 hours, followed by sintering at higher temperature of 1100°C for 2 hours. In the final step sample was cooled down to room temperature and homogenized in a mortar.

Crystal structure of the powder was studied at ambient temperature by Automated Multipurpose X-ray Diffractometer (XRD) With Guidance Software (Rigaku SmartLab, Japan). The measurement was recorded over the 10°-90° range, with 0.02° step size and 10°/min counting time. Relevant results of the structural analysis were obtained using PDXL2-Integrated X-ray Powder Diffraction Software.

The morphology of the samples was characterized by a field emission gun TESCAN MIRA3 scanning electron microscope. Before the observation, the samples were coated with a thin layer of Au using a standard sputtering technique (Polaron SC502 - Fison Instruments, UK). Transmission electron microscope images were obtained using a TEM Philips CM-20 SuperTwin operating at 160 kV with an optical resolution of 0.25 nm.

Steady-state luminescence measurements were performed using a spectrofluorometric system-Fluorolog-3 with FluorEssence™ software (Model 221, Horiba Scientific) equipped with a 450 W CW Ozone-free Xenon arc lamp as an excitation source, and Photomultiplier R928P detector. The temperature-dependent photoluminescent spectra were recorded from 200 K to 450 K using MicroOptik nitrogen cooled heating-cooling stage for temperature control.

1.2. Phase & Morphological analysis

The X-ray diffraction (XRD) analysis of the YAG:1Er0.5Mn sample reveals a clear match with the body-centered cubic structure, specifically aligned with the *Ia* $\bar{3}d$ (230) space group, as identified by ICDD card no. 01-073-3184 (Figure 1a). This congruence indicates that the crystal structure is intact and that the sample primarily comprises the desired YAG phase, with no secondary phases detected. In the context of the YAG structure, the successful incorporation of these dopant ions can be understood through their ionic radii and local coordination environments. The ionic radius of Er³⁺ (1.004 Å) is quite comparable to that of Y³⁺ (1.019 Å), facilitating the substitution at the dodecahedral eight-fold coordinated sites within the YAG lattice. Similarly, the incorporation of Mn⁴⁺ ions (0.530 Å) into the YAG structure involves their substitution of Al³⁺ ions (0.535 Å) at the octahedral six-fold coordinated sites [2]. The close match in size leads to minimal

disruption in the overall structure, and the absence of additional phases is crucial as it confirms that the dopant ions, Er^{3+} and Mn^{4+} , have been effectively incorporated. Also, the structural integrity and phase purity observed by the XRD measurement suggest a well-optimized synthesis process, laying the foundation for further investigation into the material's functional properties. The PDXL2 software enables phase identification and Rietveld analysis to assess crystallite size (~ 23 nm) and relevant structural parameters (Inset in Figure 1a), with the initial parameters for the analysis derived from the reference [3].

The sample's morphology at the micron level is characterized by a diverse range of chunk sizes, as observed through scanning electron microscopy (SEM). (Figure 1b). Regarding the TEM micrograph (Figure 1c with the corresponding size distribution histogram as an inset) it can be seen that on the nano level this material consists of sphere-like nanoparticles with an average of 34 nm in diameter.

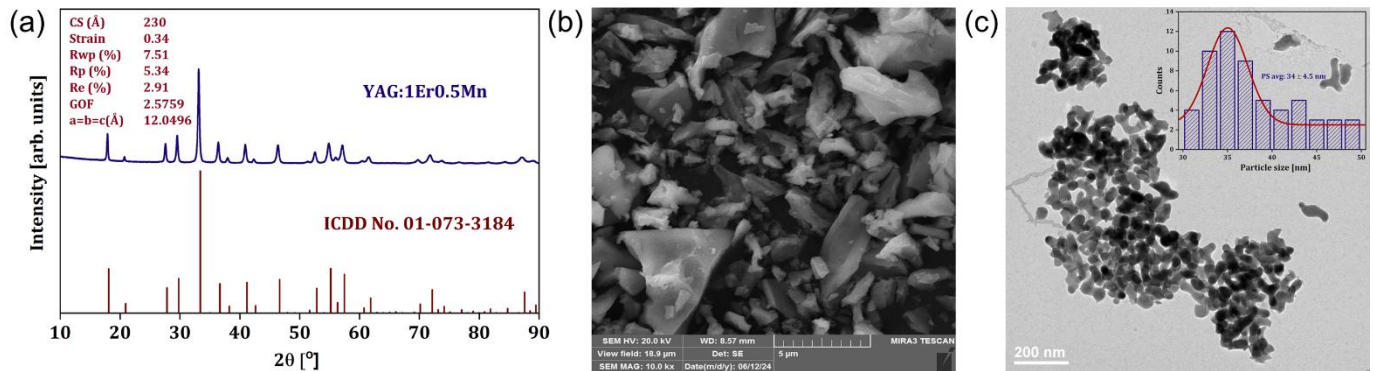


Figure 1 a) X-ray diffraction pattern of YAG:1Er0.5Mn sample. The peaks are indexed according to the ICDD card No. 01-073-3184 (CS- crystallite size, GOF-goodness of fit, Rwp – the weighted profile factor; Rp – the profile factor; Re – the expected weighted profile factor. b) Scanning electron microscopy image of the YAG:1Er0.5Mn sample recorder under 10,000× magnification. c) Transmission electron microscopy image of the YAG:1Er0.5Mn sample showing the sphere and sphere-like shaped particles.

1.3. Photoluminescence of YAG:Er³⁺/Mn⁴⁺

Photoluminescence excitation spectra of YAG:Er³⁺/Mn⁴⁺ are given in Figure a. When Mn⁴⁺ emission peaks originating from the ${}^2\text{E} \rightarrow {}^4\text{A}_2$ transition are monitored, the excitation spectrum (at $\lambda_{\text{ex}} = 670$ nm) is featured by two broad bands attributed to the excitation from the ground level of Mn⁴⁺ to the ${}^2\text{T}_{2g}$ and ${}^4\text{T}_{2g}$ levels, peaking at about 350 nm and 480 nm, respectively, matching to what was previously reported in Ref. [4]. When 555 nm emission which corresponds to the ${}^4\text{S}_{3/2} \rightarrow {}^4\text{I}_{15/2}$ is monitored, the excitation spectrum features typical sharp peaks for the Er³⁺ ion. The main excitation peak for the Er³⁺ is at about 380 nm, attributed to the ${}^4\text{I}_{15/2} \rightarrow {}^2\text{G}_{11/2}$ absorption. Conveniently, Mn⁴⁺ has an intense excitation at this wavelength, thus by irradiation by 380 nm both Er³⁺ and Mn⁴⁺ ions are being efficiently excited. Temperature-dependent emission spectra are given in Figure b. Mn⁴⁺ emission rapidly quenches with temperature increase due to its electrons being exposed to the vibrations of the host matrix. However, lanthanides have their 4f electrons shielded which is why the emissions originating from the 4f levels are almost temperature invariant up to the high temperatures. ${}^2\text{H}_{11/2} \rightarrow {}^4\text{I}_{15/2}$ emission increases with temperature at the expense of the ${}^4\text{S}_{3/2} \rightarrow {}^4\text{I}_{15/2}$ emission, which slowly drops in intensity. These two levels are thermalized, thus the electrons from the ${}^4\text{S}_{3/2}$ level get thermally excited to the ${}^2\text{H}_{11/2}$ level, in amount proportional to the temperature.

Note that in some hosts there is a red emission of Er³⁺ originating from the ${}^4\text{F}_{9/2}$ level, which would here overlap with the Mn⁴⁺ emission. This emission is weakly observed in this host when excited by 980 nm [5], and strongly when there was co-doping with Yb³⁺ ion. Thus, the red emission of Er³⁺ is pronounced with upconversion process, but negligible for the downshifting photoluminescence, as confirmed by the absence of sharp peaks in the excitation spectrum when 670 nm is observed, and disappearance of all emission at the highest temperature, while other emission of Er³⁺ is still not temperature quenched.

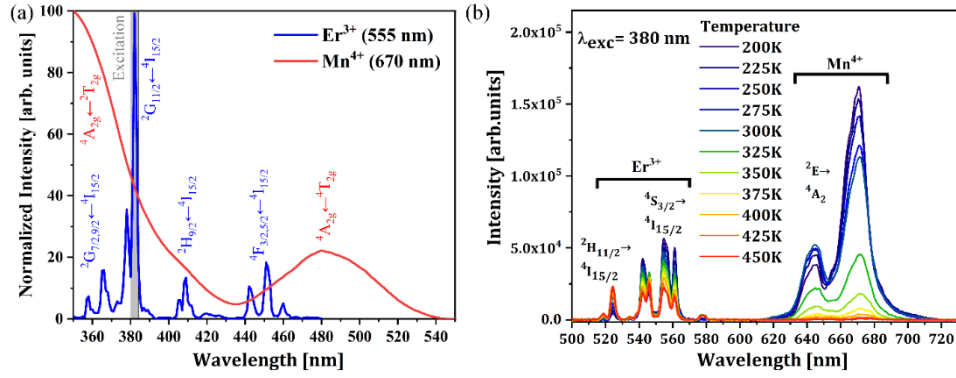


Figure 2. (a) Photoluminescence excitation spectra recorded for YAG:1Er0.5Mn sample, and (b) temperature dependent emission spectra of YAG:1Er0.5Mn excited by 380 nm.

1.4. Luminescence thermometry of YAG:Er³⁺/Mn⁴⁺

The temperature-dependent integrated emission intensities of ${}^4S_{3/2} \rightarrow {}^4I_{15/2}$ and ${}^2H_{11/2} \rightarrow {}^4I_{15/2}$ emissions of Er³⁺, and ${}^2E \rightarrow {}^4A_2$ emission of Mn⁴⁺ are given in Figure a. As the ${}^2H_{11/2}$ and ${}^4S_{3/2}$ levels are thermalized, the ratio of the optical center populations at those two levels is given by the Boltzmann distribution:

$$\frac{N({}^2H_{11/2})}{N({}^4S_{3/2})} = \frac{g({}^2H_{11/2})}{g({}^4S_{3/2})} \exp\left(-\frac{\Delta E_1}{kT}\right) \quad (1)$$

where $g = 2J+1$ is the degeneracy of the emissive energy level, and ΔE_1 is the energy difference between the thermalized levels. Thus, the luminescence intensity ratio of thermalized emissions of Er³⁺ is given by:

$$LIR_1 = \frac{I({}^2H_{11/2})}{I({}^4S_{3/2})} = \frac{N({}^2H_{11/2})A({}^2H_{11/2} \rightarrow {}^4I_{15/2})}{N({}^4S_{3/2})A({}^4S_{3/2} \rightarrow {}^4I_{15/2})} \quad (2)$$

where A is the radiative transition probability, i.e. the rate of the spontaneous emission. As the rates of the spontaneous emission depend on the Judd-Ofelt parameters and index of refraction, which are invariant of temperature, the Eq. 2 can be rewritten as:

$$LIR_1 = B_1 \exp\left(-\frac{\Delta E_1}{kT}\right) \quad (3)$$

where B_1 is the temperature-independent parameter that only depends on the properties of the host.

On the other hand, the Mn⁴⁺ and Er³⁺ levels are not thermalized and there is no apparent energy transfer between the ions. The intensity of the ${}^4S_{3/2}$ level of Er³⁺ and Mn⁴⁺ emission follow the multiphonon de-excitation and Mott-Seitz mechanisms, respectively [6]. Their intensity ratio then follows the quasi-Boltzmann distribution:

$$LIR_2 = \frac{I({}^4S_{3/2})}{I(\text{Mn}^{4+})} = B_2 \exp\left(-\frac{\Delta E_2}{kT}\right) \quad (4)$$

where ΔE_2 does not bear physical significance as in the case of the thermalized levels. Analogously is given the ratio of intensities of the ${}^2H_{11/2} \rightarrow {}^4I_{15/2}$ and ${}^2E \rightarrow {}^4A_2$:

$$LIR_3 = \frac{I\left({}^2H_{11/2}\right)}{I(\text{Mn}^{4+})} = B_3 \exp\left(-\frac{\Delta E_3}{kT}\right) \quad (5)$$

All three LIRs and the fits to the Boltzmann and quasi-Boltzmann distribution are given in Figure b. The fitted energy gap between the thermalized levels of Er³⁺ matches what is reported in the literature and what is observed in Figure b. The fitted ΔE for LIRs by Mn⁴⁺ are 4003 cm⁻¹ and 4979 cm⁻¹ by using ${}^4S_{3/2}$ and ${}^2H_{11/2}$, respectively.

The figure of merit in luminescence thermometry, the relative sensitivity, is the normalized rate of change of LIR, given by:

$$S_r [\% \text{ K}^{-1}] = \frac{1}{LIR} \left| \frac{\partial LIR}{\partial T} \right| = \frac{\Delta E}{kT} \quad (6)$$

The relative sensitivities of all three LIRs are presented in Figure c. Because intensities of Er^{3+} slowly change with temperature, the relative sensitivity of their LIR is low, but these sensors can be used even larger temperature range than measured here. However, the goal of increasing the relative sensitivity on the limited range can be done only with the rapid changes of intensities with temperature. $^4\text{S}_{3/2}$ level of Er^{3+} acts almost like the reference emission, as it is only slightly changing with temperature, and for Mn^{4+} the temperature quenching starts at room temperature, thus their LIR is rapidly changing with temperature, indicating large sensitivity. The LIR of TM and Ln^{3+} ions is already demonstrated to provide for high relative sensitivities. To increase the sensitivity further, what is needed is that the one emission in LIR increases with temperature. Until now the concept of using the thermalized emission of Ln^{3+} with the TM emission for LIR was not tested. As emission from $^2\text{H}_{11/2}$ of Er^{3+} increases with temperature and emission from ^2E level of Mn^{4+} rapidly decreases, their LIR is rapidly changing, and we have a very large relative sensitivity. It can be demonstrated that this LIR of thermalized Er^{3+} emission with the Mn^{4+} emission is equal to the product of LIR_1 and LIR_2 :

$$LIR_3 = \frac{I(^2\text{H}_{11/2})}{I(\text{Mn}^{4+})} = \frac{I(^4\text{S}_{3/2})}{I(\text{Mn}^{4+})} \frac{I(^2\text{H}_{11/2})}{I(^4\text{S}_{3/2})} = LIR_2 \cdot LIR_1 \quad (7)$$

By applying Eq. 6 to the Eq. 7, the energy difference ΔE_3 , and consequently the relative sensitivity S_r (LIR_3) is equal to the sum of ΔE_1 and ΔE_2 and their corresponding sensitivities, respectively:

$$\Delta E_3 = \Delta E_2 + \Delta E_1; \quad S_r(LIR_3) = S_r(LIR_2) + S_r(LIR_1) \quad (8)$$

This clearly shows the benefit of using thermalized emissions in combination with rapidly quenching TM emissions and demonstrates that this provides for the largest possible sensitivity for the LIR of emissions from Ln^{3+} and TM ions.

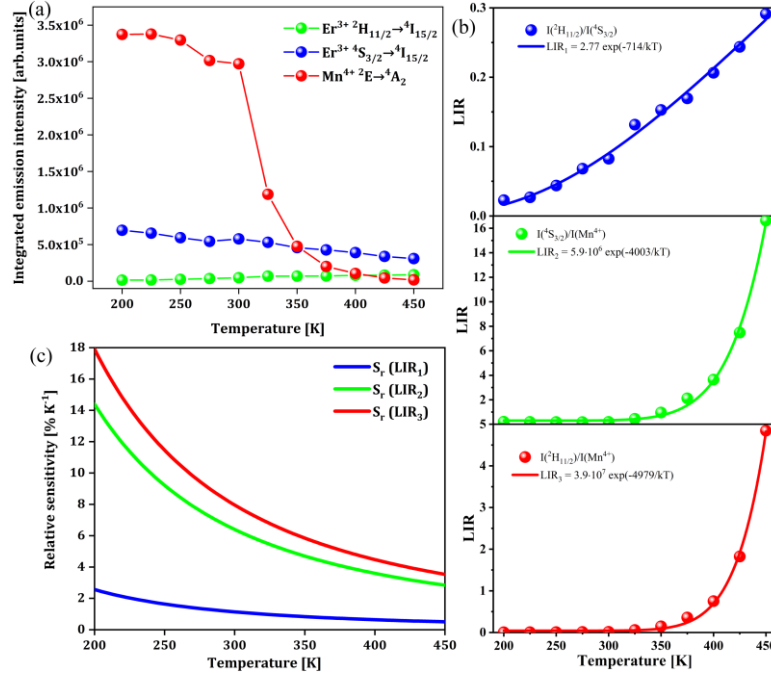


Figure 3. (a) Temperature-dependence of integrated emission intensities of transitions from $^2\text{H}_{11/2}$ and $^4\text{S}_{3/2}$ levels of Er^{3+} , and the emission of Mn^{4+} in YAG:1Er0.5Mn. (b) The combinations of luminescence intensity ratios of those 3 emissive levels, and (c) the corresponding relative sensitivities.

2. YAG:Yb³⁺/Ce⁴⁺ thermal probe

2.1. Experimental part

Following chemicals commercially available: metal nitrate salts (yttrium(III) nitrate hexahydrate, Y(NO₃)₃×6H₂O; cerium (III) nitrate hexahydrate, Ce(NO₃)₂×6H₂O; ytterbium (III) nitrate pentahydrate, Yb(NO₃)₃×5H₂O; aluminium (III) nitrate nonahydrate, Al(NO₃)₃×9H₂O; Alfa Aesar, purity 99.9%, 99.99+, 99.9%, 98+%, respectively); citric acid - CA (HOC(COOH)(CH₂COOH)₂, Sigma Aldrich, ACS reagent, ≥99.5%) and ethylene glycol - EG (HOCH₂CH₂OH, Sigma Aldrich, anhydrous, 99.8%) were used as purchased. In this work a set of six samples: Y₃Al₅O₁₂: 5 mol% Yb³⁺, Y₃Al₅O₁₂: 0.5 mol% Ce³⁺, and Y₃Al₅O₁₂:x mol% Yb³⁺, 0.5 mol% Ce³⁺ samples (x= 0.2, 1, 2.5, 5) was synthesized by Pechini method (Sample formulas and abbreviated names are given in Table 1).

Table 1. Sample formulas and abbreviated names of the synthesized YAG based samples

Sample	Sample formula	Abbreviated name
Y ₃ Al ₅ O ₁₂ :5 mol% Yb ³⁺	Y _{2.85} Yb _{0.15} Al ₅ O ₁₂	YAG:5Yb
Y ₃ Al ₅ O ₁₂ :0.5 mol% Ce ³⁺	Y _{2.985} Ce _{0.015} Al ₅ O ₁₂	YAG:0.5Ce
Y ₃ Al ₅ O ₁₂ :0.5 mol% Ce ³⁺ , 0.2 mol% Yb ³⁺	Y _{2.979} Ce _{0.015} Yb _{0.006} Al ₅ O ₁₂	YAG:0.5Ce0.2Yb
Y ₃ Al ₅ O ₁₂ : 0.5 mol% Ce ³⁺ , 1 mol% Yb ³⁺	Y _{2.955} Ce _{0.015} Yb _{0.03} Al ₅ O ₁₂	YAG:0.5Ce1Yb
Y ₃ Al ₅ O ₁₂ : 0.5 mol% Ce ³⁺ , 2.5 mol% Yb ³⁺	Y _{2.91} Ce _{0.015} Yb _{0.075} Al ₅ O ₁₂	YAG:0.5Ce2.5Yb
Y ₃ Al ₅ O ₁₂ :0.5 mol% Ce ³⁺ , 5 mol% Yb ³⁺	Y _{2.835} Ce _{0.015} Yb _{0.15} Al ₅ O ₁₂	YAG:0.5Ce5Yb

The samples have been synthesized from metal nitrates dissolved in the solution of CA and EG. Detailed method is given in the work earlier printed by our research group [1]. The acquired samples in a form of yellow gel were temperature treated in two steps: calcination at 600°C for 2 hours, followed by sintering at higher temperature of 1100°C for 2 hours. In the ultimate step samples were cooled down to room temperature and homogenized in a mortar.

2.2. Phase & Structural analysis

The X-ray diffraction (XRD) analysis of the synthesized samples reveals a clear match with the body-centred cubic structure, specifically aligned with the *Ia* $\bar{3}d$ (230) space group, as identified by ICDD card no. 01-073-3184 (Figure 4). This congruence indicates that the crystal structure is intact and that the samples comprise the desired YAG phase, with no secondary phases detected.

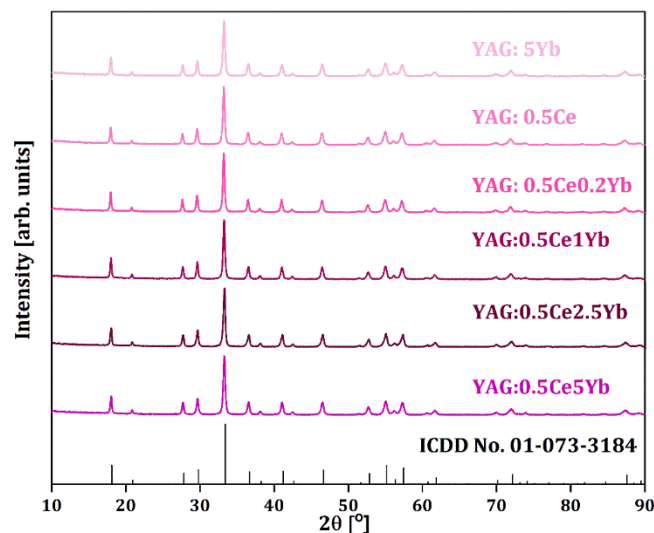


Figure 4. XRD patterns of YAG:5Yb, YAG:0.5Ce, YAG:0.5Ce0.2Yb, YAG:0.5Ce1Yb, YAG:0.5Ce2.5Yb, YAG:0.5Ce5Yb samples with the corresponding ICDD card No. 01-073-3184.

In the context of the YAG structure, the successful incorporation of these dopant ions can be understood through their ionic radii and local coordination environments. The ionic radius of Yb³⁺ (1.14 Å) and Ce³⁺ (1.143

Å) is quite comparable to that of Y^{3+} (1.019 Å), facilitating the substitution at the dodecahedral eight-fold coordinated sites within the YAG lattice [2]. The close match in size leads to minimal disruption in the overall structure, and the absence of additional phases is crucial as it confirms that the dopant ions have been effectively incorporated. Also, the structural integrity and phase purity observed by the XRD measurement suggest a well-optimized synthesis process, laying the foundation for further investigation into the material's functional properties. The PDXL2 software enables phase identification and Rietveld analysis to assess crystallite size (~ 33 nm) and relevant structural parameters, with the initial parameters for the analysis derived from the reference are presented in Table 2 [3].

Table 2. Selected structural parameters of the synthesized YAG:5Yb, YAG:0.5Ce YAG:0.5Ce0.2Yb, YAG:0.5Ce1Yb, YAG:0.5Ce2.5Yb, YAG:0.5Ce5Yb samples. CS – Crystallite size; Rwp – the weighted profile factor; Rp – the profile factor; Re – the expected weighted profile factor; and GOF – the goodness of fit.

ICDD 01-073-3184	YAG:5Yb	YAG:0.5Ce	YAG:0.5Ce0.2Yb	YAG:0.5Ce1Yb	YAG:0.5Ce2.5Yb	YAG:0.5Ce5Yb
CS (Å)	299(7)	305(7)	354 (8)	351(9)	346(10)	343(9)
Strain	0.34 (3)	0.31 (4)	0.31 (2)	0.32(2)	0.36(3)	0.35(3)
GOF	1.1520	1.1660	1.2150	1.1453	1.1745	1.1643
Rwp (%)	8.98	9.21	9.33	8.81	9.08	9.27
Rp (%)	6.74	7.07	7.13	6.64	6.88	7.03
Re (%)	7.79	7.89	7.04	7.69	7.73	7.68
a=b=c	12.0171(8)	12.0200(13)	12.0279(8)	12.0178(12)	11.9984(7)	12.0169(9)

1.1. UV-VIS diffuse reflectance of YAG:Yb³⁺/Ce⁴⁺

UV-vis-NIR diffuse reflectance spectra of YAG:5Yb, YAG:0.5Ce YAG:0.5Ce0.2Yb, YAG:0.5Ce1Yb, YAG:0.5Ce2.5Yb, YAG:0.5Ce5Yb samples recorded at room temperature are presented in Figure 5. The absorption bands in the short wavelength range around 460 nm correspond to the Ce³⁺ absorptions from the 4f to 5d₁ excited level. The absorption band visible at the long wavelengths around 970 nm is due to the Yb³⁺ ²F_{7/2} to ²F_{5/2} transition.

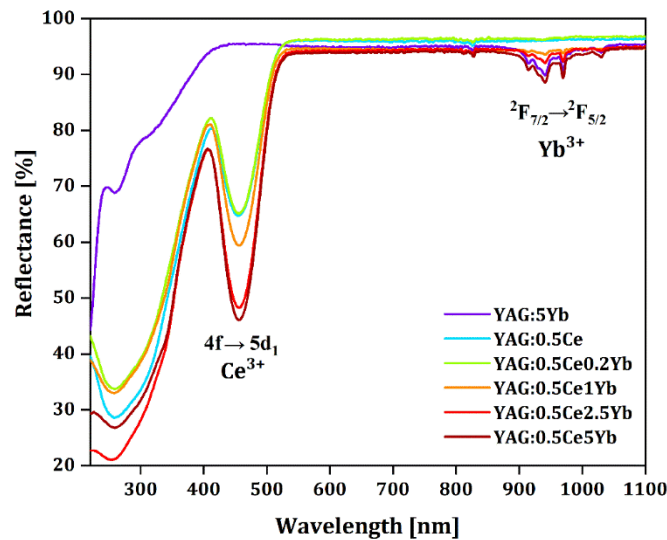


Figure 5. UV-vis-NIR diffuse reflectance spectra of YAG:5Yb, YAG:0.5Ce YAG:0.5Ce0.2Yb, YAG:0.5Ce1Yb, YAG:0.5Ce2.5Yb, YAG:0.5Ce5Yb samples.

All activities led to the **formal completion of Milestone 1.2: High-performance luminescence thermal probes selected**, as outlined in the project plan. The list is as follows:

1. GdVO₄ colloidal nanoparticles doped with europium (Eu³⁺)
2. LaPO₄ colloidal nanoparticles doped with europium (Eu³⁺)
3. YVO₄ colloidal nanoparticles doped with europium (Eu³⁺)

References

- [1] J. Periša, Z. Ristić, W. Piotrowski, Ž. Antić, L. Marciniak, M.D. Dramićanin, "All near-infrared multiparametric luminescence thermometry using Er³⁺, Yb³⁺-doped YAG nanoparticles," *RSC Adv.* **11** (2021) 15933–15942. <https://doi.org/10.1039/D1RA01647D>.
- [2] R.D. Shannon, "Revised effective ionic radii and systematic studies of interatomic distances in halides and chalcogenides," *Acta Crystallogr. Sect. A* **32** (1976) 751–767. <https://doi.org/10.1107/S0567739476001551>.
- [3] D. Rodic, M. Mitric, R. Tellgren, H. Rundlof, "The cation distribution and magnetic structure of Y₃Fe_(5-x)Al_xO₁₂," *J. Magn. Magn. Mater.* **232** (2001) 1–8. [https://doi.org/10.1016/S0304-8853\(01\)00211-6](https://doi.org/10.1016/S0304-8853(01)00211-6).
- [4] J. Jiang, Y. Cheng, W. Chen, Z. Liu, T. Xu, M. He, L. Zhou, R. Yuan, W. Xiang, X. Liang, "Mn⁴⁺/Zn²⁺:YAG glass ceramic for light emitting devices," *Mater. Res. Bull.* **105** (2018) 277–285. <https://doi.org/10.1016/j.materresbull.2018.05.003>.
- [5] E. Cavalli, L. Esposito, J. Hostaša, M. Pedroni, "Synthesis and optical spectroscopy of transparent YAG ceramics activated with Er³⁺," *J. Eur. Ceram. Soc.* **33** (2013) 1425–1434. <https://doi.org/10.1016/j.jeurceramsoc.2013.01.012>.
- [6] A. Ćirić, M.D. Dramićanin, "LumTHools - Software for fitting the temperature dependence of luminescence emission intensity, lifetime, bandshift, and bandwidth and luminescence thermometry and review of the theoretical models," *J. Lumin.* **252** (2022) 119413. <https://doi.org/10.1016/j.jlumin.2022.119413>.